Shock consolidation of diamond and graphite mixtures to fused polycrystalline diamond

David K. Potter and Thomas J. Ahrens
Seismological Laboratory, California Institute of Technology, Pasadena, California 91125

(Received 29 May 1987; accepted for publication 9 September 1987)

The production of fused compacts of polycrystalline diamond was achieved by subjecting porous (35%–49% porosity) mixtures of diamond crystals plus graphite (13–16 wt. %) to dynamic shock pressures of 10–18 GPa. The recovered material from an initial mixture of 4–8-μm diamond crystals plus graphite revealed a very homogeneous texture with little evidence of original grain boundaries. The preconsolidation addition of graphite also allowed ultrafine ($<5\,\mu$m) diamond crystals to be consolidated; this was not previously possible with the use of diamond crystals alone. The results are consistent with calculations which suggest that a thin layer of graphite surrounding a diamond crystal delays thermal equilibrium between the surface and interior of the diamond crystal, thus allowing greater surface heating. Consolidation is also probably enhanced by conversion of graphite to diamond, possibly via the liquid state.

I. INTRODUCTION

Previous experiments[1] showed that the production of a fused polycrystalline solid compact, by subjecting an initially porous aggregate of diamond crystals to moderate dynamic shock stress, depended critically on the size of the initial crystals. Ultrafine crystals ($<5\,\mu$m) did not fuse together, and it was assumed that this result was due to the fact that the time constant for thermal equilibrium between the surface and interior of the crystals approached the shock transit time through them, thus preventing local surface melting and consolidation. In the present study we describe the results of experiments which have shown that the initial addition of small quantities of very fine graphite to samples containing diamond crystals can be used to (a) consolidate fine diamond crystals and (b) produce more homogeneous fusion between larger diamond crystals (4–8 μm). We will show through model calculations that a thin layer of graphite covering diamond crystals effectively delays thermal equilibrium between the surface and interior of the crystals (because of the lower thermal diffusivity of graphite, as compared to diamond), thus allowing greater surface heating.

II. PHASE DIAGRAM OF CARBON

The details of the diamond/graphite equilibrium line have been known for some time, both from theoretical considerations[2,3] and experimental synthesis of diamond from graphite.[4] However, the exact nature of the melting lines of graphite and diamond have only recently begun to emerge. Venkatesan *et al.*[5] and Braunstein *et al.*[6] melted graphite with a pulsed ruby laser at pressures of less than 0.1 GPa, and all experiments indicated a melting temperature of about 4300 K. In addition, the latter study indicated that the liquid evaporates at about 4700 K. The details of the slope of the melting line at higher pressures remains more controversial. Van Vechten[7] used electronegativity as a scaling parameter to construct universal phase diagrams for group IV elements and binary alloys crystallizing in the diamond structure. His results for carbon are shown in Fig. 1(a) and predict that the melting line should have a negative slope of about -0.07 GPa/K. Experimental evidence[8,9] showed that the melting line of diamond must come to the triple point (12.5–13 GPa, 4000–4200 K) with a slightly negative slope. Further evidence for this came from the behavior of small diamond crystals embedded in graphite rod specimens.[9] It was found that there was a sharp temperature threshold at which the diamond crystals completely graphitized. By analogy with the direct graphite to diamond transformation, the flash-heating diamond graphitization line would be expected to be parallel to the diamond melting line, but a few hundred degrees cooler, and thus the slope of the line just above the triple point was inferred from that of the flash-heat diamond graphitization line.

Recently, Shaner *et al.*[10] measured the sound velocity of graphite shocked into the high-pressure diamond field. These results are consistent with a phase diagram in which carbon (diamond) remains solid from 80 to 140 GPa along the Hugoniot curve. A calculated pressure-temperature Hugoniot curve[11] along with the data points of Shaner *et al.* is also shown in Fig. 1(a). Shaner *et al.* did not find evidence for a melting transition at any of these points, suggesting that the melting curve has a positive slope at high pressure. In Fig. 1(b) we present a proposed phase diagram for carbon which is basically an updated version of that developed by Bundy[8] constrained by these recent observations and theory.

III. EXPERIMENTAL DETAILS

Shock compaction was achieved by using the flyer plate-type shock-wave generator and momentum trap recovery system shown in Fig. 2, which is a modified version of that given by Ahrens *et al.*[12] A stainless-steel impactor plate (1.6 cm in diameter and 0.25 cm thick) was accelerated to a velocity of between 1.81 and 1.87 km/s and impacted against a stainless-steel sample capsule containing the diamond crystals plus graphite sample which had been pressed into the sample ring and capsule. This produced a shock pulse with a duration of $\sim 0.8\,\mu$s. A 0.05-cm-thick disk (single crystal) of Al_2O_3 (sapphire) was placed between the stainless-steel and diamond crystals (at the interface nearest to where the

 0021-8979/88/030910-05$02.40

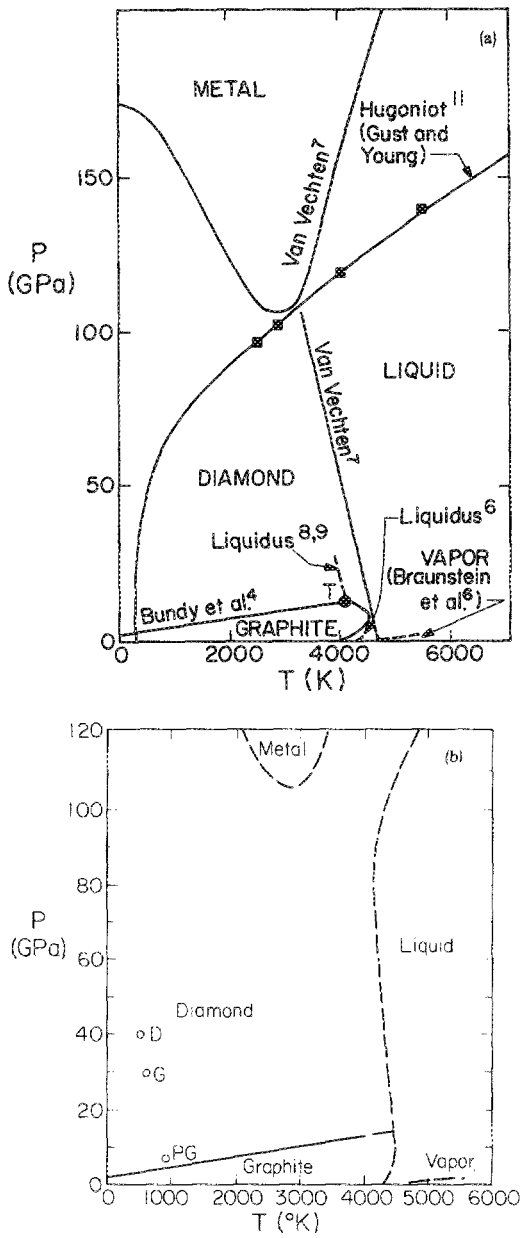

FIG. 1. Phase diagram of carbon. (a) Data which constrain phase diagram based on indicated references. (b) Proposed phase diagram of carbon. Values of P_H and T_H from Table II are shown for single-crystal diamond *D*, single-crystal graphite *G*, and porous graphite *PG*.

flyer plate impacts) so as to act as an umbrella to prevent molten metal spray from the stainless steel interacting with the sample. The initial sample was prepared by mixing diamond crystals and graphite until a uniform color tone was achieved. This ensured that substantially all of the diamond crystals were coated with graphite. The experimental conditions are given in Table I.

IV. EXAMINATION OF RECOVERED SAMPLES

A. Successful fused compacts

1. Synthetic diamond crystals (<5 μm) plus graphite (Fig. 3)

Material from shot 909 was well consolidated, and scanning electron microscopy (SEM) analysis showed evidence

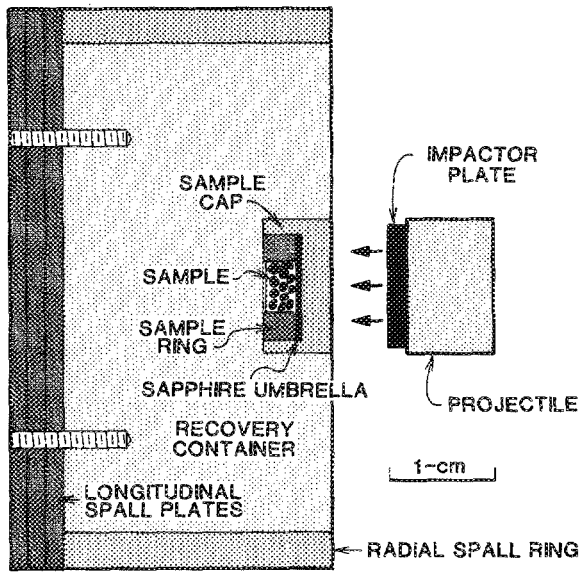

FIG. 2. Shock compaction of diamond experimental assembly.

of fusion between diamond crystals [Fig. 3(c)]. This result contrasted to material recovered from previous experiments in which we unsuccessfully attempted to consolidate powdered <5-μm diamond crystals alone.[1] The previous samples were very unconsolidated and showed no evidence of fusion.

2. Synthetic diamond crystals (4–8 μm) plus graphite (Fig. 4)

SEM analysis of the material recovered from shot 908 revealed a very homogeneous texture, with little evidence of original crystal boundaries [Fig. 4(b); compare this with the initial crystals, Fig. 4(a)], much more so than previous compacts where the starting material was the 4–8-μm diamond crystals alone.[1] However, the strength of the compact appeared to be slightly weaker than those recovered in the previous work.

B. Partially fused compact: Natural diamond crystals (100–150 μm) plus graphite

Analysis of the material recovered from shot 886 revealed a high degree of fracturing within the individual crystals [Fig. 5(b)], as was the case for previous compacts formed from large diamond crystals without graphite,[1] and there was little evidence of fusion. The strength of the compact was only moderate, since particles could be removed with a steel probe.

V. X-RAY ANALYSIS

Powder x-ray diffraction was performed by the Debye–Scherrer method with the use of a Siemens D-500 diffractometer with Cu$K\alpha$ radiation. Figures 6(a) and 7(a) show diffraction patterns of the original unshocked mixtures of the <5-μm diamond plus graphite and 4–8-μm diamond plus graphite. The 002 of graphite and the 111 and 220 *d* spacings of diamond are clearly evident. Figure 6(b) shows the diffraction pattern of the shocked <5-μm diamond plus graphite sample (shot No. 909). This shows that while the

TABLE I. Experimental conditions.

Shot number	Initial sample	Initial pore volume (%)	Projectile velocity (km/s)	Recovered sample condition
886	Natural diamond crystals (100–150 μm) plus 13 wt. % graphite	35	1.81	Compacted, *no fusion*
908	Synthetic diamond (4–8 μm) plus 16 wt. % graphite	49	1.84	Fused compact homogeneous texture Substantial conversion of graphite to diamond
909	Synthetic diamond (<5 μm) plus 16 wt. % graphite	49	1.87	Compacted partial fusion Substantial conversion of graphite to diamond

diamond peaks remain, the graphite peak has substantially diminished. This suggests that much of the graphite has converted to diamond. The diffraction pattern of the shocked 4–8-μm diamond plus graphite sample from shot No. 908 [Fig. 7(b)] also exhibits a much diminished graphite peak. Moreover, the broadening of the diamond (111) peak implies the presence of very small crystallite sizes (10–20 nm). The Al_2O_3 peaks shown in this figure were due to small amounts of the remains of the Al_2O_3 disk which were unavoidably removed, along with the diamond, during the course of extracting a part of the sample for the analysis.

VI. MODEL CALCULATIONS

A. Continuum thermodynamics

By using the shock (U_s) and particle (u_p) velocity relationship of Pavlovskii[13] for single-crystal diamond (3.51 Mg/m^3),

$$U_s\,(\mathrm{km/s}) = 12.16 + 1.00u_p, \tag{1}$$

the shock pressure (P_H) generated in single-crystal diamond, after passage of the shock wave through stainless-steel 304 and an Al_2O_3 single crystal, was estimated by using the impedance matching technique.[14,15] The projectile velocity was taken to be 1.82 km/s. The subsequent value of P_H generated in graphite (after passage of the shock wave through single-crystal diamond) was then calculated. Values were obtained for both single-crystal (2.26 Mg/m^3) and porous graphite (initial density 55% of the crystal density) by using the following shock and particle velocity relationship:

$$U_s\,(\mathrm{km/s}) = 4.3 + 1.8u_p, \tag{2}$$

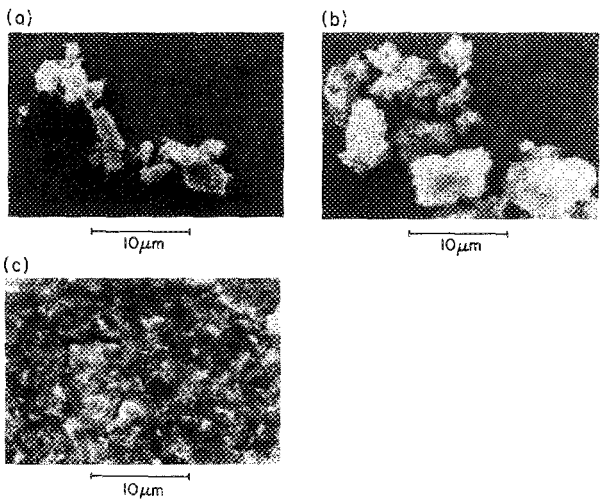

FIG. 3. Scanning electron images (a) unshocked <5-μm synthetic diamond; (b) unshocked graphite; (c) fused compact (shot No. 909).

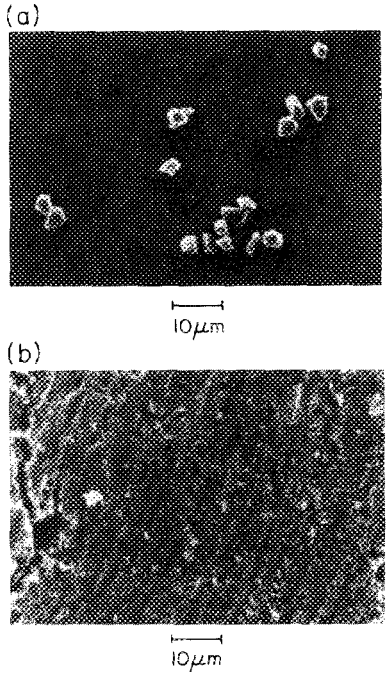

FIG. 4. Scanning electron images: (a) unshocked 4–8-μm diamond crystals; (b) fused compact formed from 4–8-μm diamond crystals plus graphite (shot No. 908).

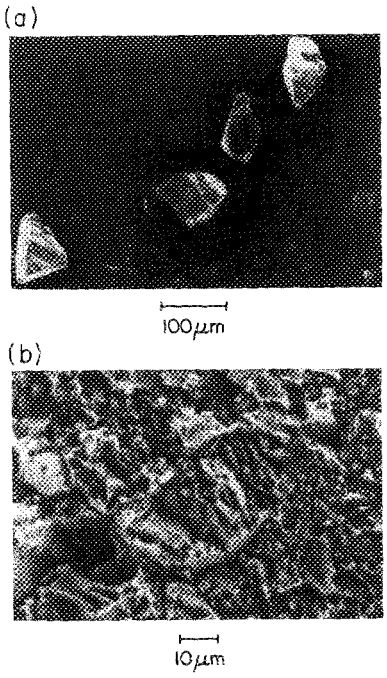

FIG. 5. Scanning electron micrographs illustrating (a) unshocked 100–150-μm natural diamond crystals and (b) compact formed from diamond crystals plus graphite (shot No. 886).

with the use of data from Marsh[16] for values of u_p in the range 0–2 km/s.

The shock (continuum) temperature T_H was given by[14]

$$T_H = T_s + V_H(P_H - P_s)/\gamma C_v, \tag{3}$$

where T_s and P_s are the temperature and pressure along the principal isentropes, V_H is the high-pressure specific volume, γ is the Grüneisen parameter (taken to be 0.9),[13] and C_v is the specific heat at constant volume (assumed to be $3R/M$, where R is the gas constant and M is the atomic weight).

Values of T_H are given in Table II and plotted in Fig. 1(b). The results indicate that higher temperatures are generated in the graphite (particularly if it is porous), but these

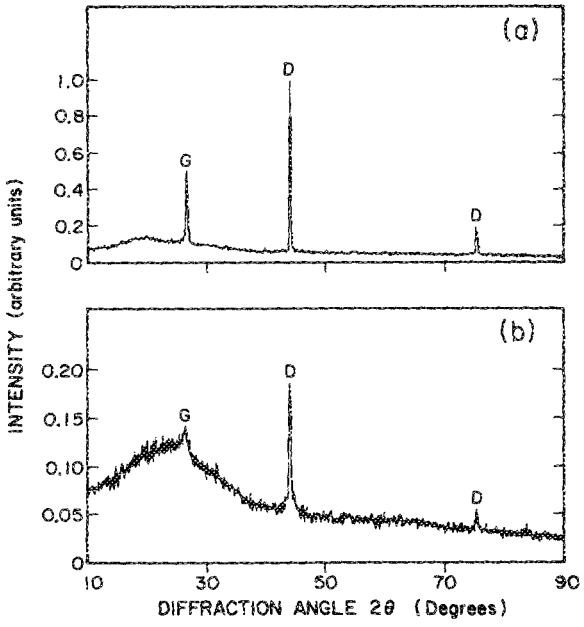

FIG. 6. Debye–Scherrer diffraction patterns, shot 909: (a) initial graphite (G) plus diamond (D) mixture; (b) postshock pattern.

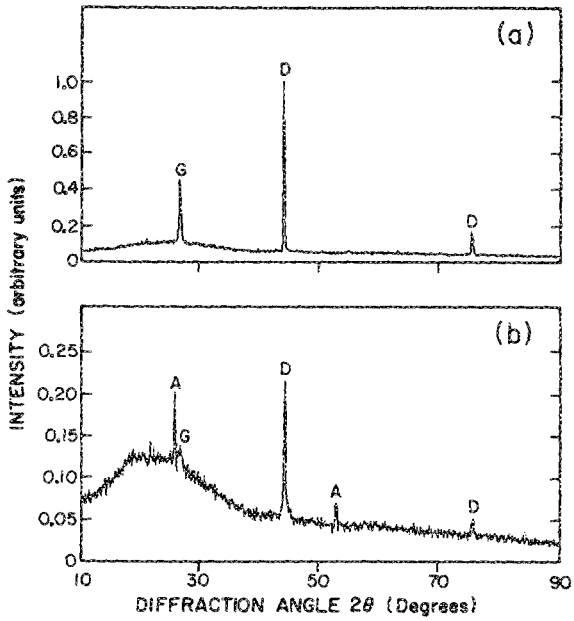

FIG. 7. Debye–Scherrer diffraction patterns, shot 908: (a) initial graphite (G) plus diamond (D) mixture; (b) postshock pattern. A indicates sapphire diffraction peak.

are only a few hundred degrees higher than those generated in the diamond and well below those required for melting. Since these temperatures are some 3000 K below the melting line of diamond, we conclude they are absolute lower bounds and that achievement of higher temperatures can only be the result of local inhomogeneous heating. This concept was suggested by De Carli[17] for the shock production of diamond from initially porous graphite. We assume that grain-boundary sliding is the main mechanism for generating the necessary temperatures to produce partial melting in the fused compacts. However, jetting and irregular reflection probably also occur. Note that under the above conditions, graphite is shocked into the diamond regime.

B. Time scales for heat flow

There are at least three time scales of interest which may be calculated with simple one-dimensional assumptions in

TABLE II. Shock pressures and continuum temperatures generated in single-crystal diamond and graphite samples. Values for the graphite samples represent those determined after passage of the shock wave through single-crystal diamond. Projectile velocity in each case was 1.82 km/s.

Sample	Shock pressure P_H[a] (GPa)	Shock temperature T_H (K)
Single-crystal diamond (3.51 g/cm^3)	40.0	500
Single-crystal graphite (2.26 g/cm^3)	29.6	610
Porous graphite 55% of single-crystal density	7.0	910

[a] Initial shock states.

the present experiments. These are (1) the time scale of freezing of a layer of L mass fraction of molten material, t_f; (2) the time scale required to heat and melt, via frictional sliding or other mechanisms on the surface and Fourier conduction into the interior, the entire crystallite then achieving an approximately uniform temperature, t_t; and (3) the time scale of shock-wave propagation through the crystal, t_s. The latter time scale t_s that we might infer may be on the order of the period of frictional heating of the surface, although other processes such as jetting and irregular reflection may also assist in production of melt.

The time scale for freezing, t_f, an initially molten layer of mass fraction L [12] is given by the theory of Schwarz *et al.*[18] as

$$t_f = \pi D/16\,[LdH_m/D\,C_p(T_m - T_0)]^2, \tag{4}$$

where D is the thermal diffusivity of diamond,[19] ($\sim 1\times 10^{-4}$ m^2/s), d is crystal diameter, H_m is the estimated heat of fusion[7] (9.2 MJ/kg); C_p is the specific heat at constant pressure[20] (2 kJ/(kg K), and $(T_m - T_o)$ is the temperature difference between melting and ambient temperature (4000 K). For $d\sim 10\ \mu$m and $L = 0.05$, $t_f = 6.5\times 10^{-10}$ s. This time is very short compared to the thermal equilibrium time which from

$$t_t \sim d^2/D \tag{5}$$

is $\sim 10^{-6}$ s. However, the value of t_f is comparable with the shock transit time t_s through a 10-μm crystallite given by

$$t_s = d/U_s, \tag{6}$$

where we assume a mean shock velocity of ~ 15 km/s. This size range of crystal appears to shock consolidate best either with graphite or without.[1] As noted earlier,[1] when the initial crystallite size becomes small, the value of $t_t \to t_s$, and we infer that the crystals conduct heat from the surface so rapidly that they become nearly isothermal. (Shock welding appears not to occur in < 5-μm crystals without graphite under our experimental conditions.) The critical crystallite diamond value obtained from setting $t_s = t_t$ is 0.007 μm.

As partial fusion of the fine, < 5-μm sample is observed (shot 909, Table I), two mechanisms are expected to be at work, causing enhanced fusion of the diamond crystals. We believe that as graphite is a good thermal insulator, with respect to diamond with $D\sim 10^{-6}$ m^2/s it provides a thermal insulating layer between diamond crystals during shock consolidation, and this allows more of the diamond surface to be heated to the melting point during compaction. For example, a 0.1-μm-thick layer of graphite around a 10-μm diamond crystal will have a thermal equilibrium time of $\sim 10^{-8}$ s; this is much longer than the freezing time of 6.5×10^{-10} s calculated from Eq. (4). In addition, some of the graphite appears to convert to diamond, possibly partially from the liquid state. Substantial, but not complete, conversion from graphite to diamond is demonstrated in Figs. 6 and 7.

VII. CONCLUSIONS

We conclude that mixing a small quantity of graphite with diamond upon shock consolidation effectively delays thermal equilibrium between the surface and interior of the diamond crystals and allows greater surface heating and hence shock consolidation. This is consistent with the experimental results of (a) the consolidation of ultrafine (< 5 μm) diamond crystals plus graphite, in contrast to previous experiments where the diamond crystals alone did not consolidate, (b) the increased homogeneity of the 4–8-μm diamond crystals plus graphite recovered sample over previous compacts formed from 4–8-μm crystals alone, and (c) the increased enhancement of shock consolidation for larger (100–150 μm) diamond crystals, when initially mixed with graphite.

ACKNOWLEDGMENTS

This work was supported by the National Science Foundation and under the Program for Advanced Technologies at the California Institute of Technology, supported by TRW, GTE, General Motors, and Aerojet General, Contribution No. 4463, Division of Geological and Planetary Sciences. We appreciate the help of Dr. John Armstrong and Cheryl Brigham in obtaining SEM images and are grateful to an anonymous reviewer for helpful comments.

[1] D. K. Potter and T. J. Ahrens, Appl. Phys. Lett. **51**, 317 (1987).
[2] F. D. Rossini and R. S. Jessup, J. Res. Natl. Bur. Stand. U.S. **21**, 491 (1938).
[3] R. Berman and F. Simon, Z. Elektrochem. **59**, 33 (1955).
[4] F. P. Bundy, J. Chem. Phys. **38**, 631 (1963).
[5] D. C. Venkatesan, J. M. Jacobson, B. S. Gibson, G. Elman, G. Braunstein, M. S. Dresselhaus, and G. Dresselhaus, Phys. Rev. Lett. **53**, 360 (1984).
[6] G. Braunstein, J. Steinbeck, M. S. Dresselhaus, G. Dresselhaus, B. S. Elman, T. Venkatesan, B. Wilkens, and D. G. Jacobsen, *Proceedings of the Materials Research Society (Boston)*, edited by H. Kurz, G. L. Olson, and J. M. Poate (Materials Research Society, Pittsburgh, PA, 1986), Vol. 51, p. 233.
[7] J. A. Van Vechten, Phys. Rev. B **7**, 1479 (1973).
[8] F. P. Bundy, J. Geophys. Res. **85**, 6930 (1980).
[9] F. P. Bundy, J. Chem. Phys. **38**, 618 (1963).
[10] J. W. Shaner, J. M. Brown, C. A. Swenson, and R. G. McQueen, J. Phys. (Paris) Colloq. **45**, C8-235 (1984).
[11] W. H. Gust and D. A. Young, in *High Pressure Research and Technology*, edited by K. D. Timmerhaus and M. S. Barber (Plenum, New York, 1979).
[12] T. J. Ahrens, D. Kostka, P. Kasiraj, T. Vreeland, Jr., A. W. Hare, F. D. Lemkey, and E. R. Thompson, *Rapid Solidification Processing Principles and Technologies, III*, edited by R. Mehrabian (National Bureau of Standards, Washington, DC, 1983), p. 672.
[13] M. N. Pavlovskii, Sov. Phys. Solid State **13**, 741 (1971).
[14] T. J. Ahrens, in *Methods of Experimental Physics*, edited by C. Sammis and T. L. Henyey (Academic, New York, in press).
[15] W. H. Gourdin, Prog. Mat. Sci. **30**, 39 (1986).
[16] S. P. Marsh, ed., *LASL Shock Hugoniot Data* (University of California Press, Berkeley, CA, 1980).
[17] P. S. De Carli, in *High Pressure Science and Technology*, edited by K. D. Timmerhaus and M. S. Barber (Plenum, New York, 1979), Vol. 1, pp. 940–943.
[18] R. B. Schwarz, P. Kasiraj, T. Vreeland, Jr., and T. J. Ahrens, Acta Metall. **32**, 1243 (1984).
[19] S. P. Clark, Jr., in *Handbook of Physical Constants*, edited by S. P. Clark, Jr. (Geol. Soc. Am. Mem., 1966), Vol. 97, p. 459.
[20] R. A. Robie, B. S. Hemingway, and J. R. Fisher, U. S. Geo. Survey Bull. No. 1452 (1978).